

VIII International Conference on Computational Methods for Coupled Problems in Science and Engineering  
COUPLED PROBLEMS 2019  
E. Oñate, M. Papadrakakis and B. Schrefler (Eds)

## CFD SIMULATION OF EVAPORATING ELECTRICALLY CHARGED SPRAYS IN FOOD CHILLING WAREHOUSES – COUPLED PROBLEMS 2019

A. Brentjes\*, A.Pozarlik<sup>†</sup> and G.Brem<sup>†</sup>

<sup>\*†</sup>Thermal Engineering Group, faculty of Engineering Technology  
University of Twente  
P.O. Box 217, 7500AE Enschede, The Netherlands  
e-mail: a.brentjes@utwente.nl, web page: <http://www.utwente.nl/ctw/thw/>

**Key words:** CFD, Charged Sprays, Food Chilling, Evaporation

**Abstract.** A potential novel application for electrically charged (water) spray is to improve cooling efficiency and reduce moisture loss in food chilling warehouses. In this paper we work toward a numerical (CFD) model that can be used to investigate the viability of this application. We build a simplified model which considers the spray droplets as inert particles and compare simulation results with data from literature. This model is then extended to include the effects of evaporation, which plays an important role in cooling and heat transfer.

### 1 INTRODUCTION

Electrostatic charging of spray droplets and particles is a well known method for improving the transfer efficiency of spraying systems. Electrostatic spraying systems are therefore good technological solutions when the spray material is expensive, or overspray is highly undesirable, and are used commonly in spray painting and agricultural pesticide application<sup>[1]</sup>. The present research aims to investigate a new application for charged sprays: chilling warehouses in food industry. Spraying water in a chilling warehouse has two purposes; it counteracts the drying effect of cold air on warm products, and provides additional evaporative cooling effort. High transfer efficiencies are required in this application, because excess moisture will condense and freeze in the evaporators. This makes it a potentially interesting application for charged sprays.

In this paper we work towards a Computational Fluid Dynamics simulation of a charged-spray-assisted chilling warehouse. The use of computer simulations to investigate this application is an obvious choice, given the costs involved with refitting entire production lines. It is however not straightforward, given the wide range of involved physical processes that need to be modelled efficiently and accurately.

Numerical simulation of charged sprays is not new in general. The scope of such simulations is however often limited based on the application case. In works on spray painting the spray droplets are often treated as inert particles, disregarding the effects of evaporation and heat transfer<sup>[2, 3, 4]</sup>. Arumugham-Achary et al.<sup>[5]</sup> provide a good framework for a model that includes evaporation, but focuses on a small-scale use case and does not consider droplet charging. Several works on electrostatic precipitators<sup>[6, 7]</sup> do cover particle charging, but not discharging or evaporation. In the cooling application all these physical phenomena are relevant. This is why we aim to build a simulation that includes all these physical models, and can solve large scale problems.

The first step toward the complete model is a simulation that can simulate charged, inert particles, which is validated against results from literature. We choose to replicate the simulation and measurements by Domnick et al.<sup>[2]</sup> to validate the model. Hence, the geometry and conditions that we simulated have been adapted from their work.

## 2 THEORY

The CFD model for the validation case needs to consider three “phases”. These are the gas, the droplets, and the electric field. The droplet phase interacts bi-directionally with the airflow and the electric field, but the airflow and the electric field are not directly connected. The governing equations for these phases, and how the interactions are modelled are described below.

### 2.1 Gas

The gas is assumed to be incompressible and isothermal, and is therefore governed by the continuity equation and the Navier-Stokes equations. Since the droplet phase will be exchanging momentum with the gas phase through drag, a reaction term must be added to the momentum equations. This reaction is implemented in the form of a volumetric force, i.e. a momentum source. The resulting formulation for the momentum equations is shown in equation (1).

$$\rho \left( \frac{\partial \vec{u}}{\partial t} + \vec{u} \cdot \vec{\nabla} \vec{u} \right) = -\vec{\nabla} p + \mu \nabla^2 \vec{u} + \vec{f}_d \quad (1)$$

Here  $\vec{f}_d$  is the volumetric drag force, positive in the direction of the force acting on the gas phase.

### 2.2 Droplets

The droplets are, in the validation case, treated as inert particles. The motion of any single droplet is the result of the sum of forces acting upon it, according with Newton's

laws. In this case three forces are considered; drag, gravity and electrostatic force. The acceleration of a droplet/particle can be formulated as in equation (2).

$$\frac{d\vec{u}_p}{dt} = \frac{3}{4} \frac{\rho C_D}{\rho_p d_p} |\vec{u} - \vec{u}_p| (\vec{u} - \vec{u}_p) + \frac{\vec{g}(\rho_p - \rho)}{\rho_p} + \frac{6}{\pi d_p^3} \frac{q_p \vec{E}}{\rho_p} \quad (2)$$

Here  $C_D$  denotes the drag coefficient of the droplet,  $\vec{E}$  denotes the local electric field and  $q_p$  the droplet charge.

### 2.3 Electric field

Although not typically considered to be a fluid “phase”, the electric field can be treated as such. The electric field is assumed to be static, and can therefore be written as the gradient of an electric potential:  $\vec{E} = -\vec{\nabla}\Phi$ . The electric potential satisfies Poisson’s equation, see equation (3).

$$\vec{\nabla} \cdot \vec{E} = -\nabla^2 \Phi = \frac{\rho_q}{\epsilon_0} \quad (3)$$

Here  $\rho_q$  denotes the local volumetric charge density and  $\epsilon_0$  the permittivity of vacuum.

### 2.4 Coupling

The gas flow and electric field equations treat the solution as a continuum, while the droplets are treated as (point-)particles with discrete properties. Coupling these requires the use of control volumes, i.e., a computational grid. The strength and direction of the momentum source  $\vec{f}_d$  in equation (1) is determined by taking the sum of the drag forces experienced by all particles inside the control volume, and dividing by the volume. Similarly, the charge density  $\rho_q$  in equation (3) is the sum of the droplet charges  $q_p$  in the grid cell divided by the volume.

## 3 NUMERICAL METHOD

For this simulation we have chosen to use the commercial Ansys Fluent code (version 18) as the CFD solver. The models necessary to compute the electrostatic potential and electrostatic force are implemented using so-called “User Defined Functions” (UDFs).

The validation problem is a steady state case, which means a RANS approach can be used for modelling the fluid flow. The droplets are modelled using a Lagrangian approach, which facilitates the implementation of evaporation modelling. A Lagrangian approach does not allow for true steady state modelling, so instead a quasi-steady approach is taken. Each tracked parcel represent a mass flow rather than a discrete mass of particles, and the parcel locations are represented by trajectory lines instead of points. Due to the disperse nature of the spray and electrostatic repulsion between droplets, droplet collision

and coalescence can be neglected, and are not modelled.

### 3.1 Solver sequence

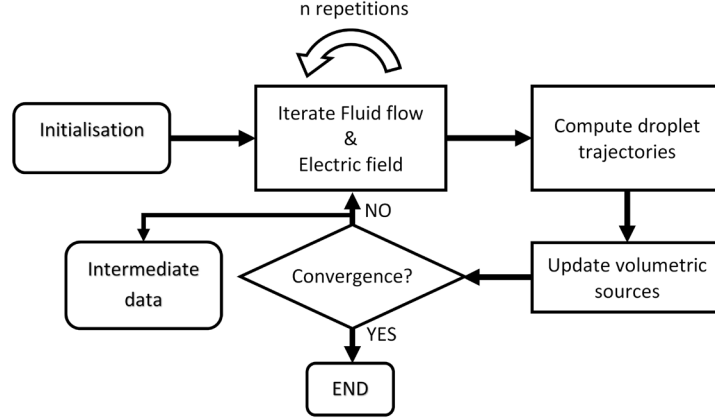


Figure 1: The process flow of the solver

Figure 1 illustrates the process flow of the solver. After initialisation the Eulerian solver is run, calculating the gas flow and the electric field. Then, droplets are injected and their trajectories are calculated, using the flow data from the previous step. Based on the droplet trajectories the volumetric source fields, representing the drag force acting on the fluid and the electric charge density, are updated. If the solution is converged the solver is stopped, otherwise intermediate data is recorded and the steps are repeated.

### 3.2 Continuous phase model

To obtain a steady state solution for a turbulent flow we solve the Reynolds-averaged Navier-Stokes equations. The  $k-\epsilon$  turbulence model is used to close the model, as done in many preceding works<sup>[2, 3, 5]</sup>.

### 3.3 Particle tracking

The droplets are modelled using a quasi-steady Lagrangian approach. This means that parcels of droplets are injected in between fluid flow iterations, and their trajectories are integrated until they impact the target or leave the domain through an outlet. Each of the calculated trajectories represents a “continuous” flow of particles of a specific diameter and charge. The amount of particles per trajectory is represented as a so-called strength, or mass flow per second.

To account for electrostatic repulsion between droplets a two-way interaction with the electric field model is used. The electric field applies a force to the droplets, while the charge of the droplets acts as the source term seen in equation (3), influencing the

electric field. Because the electric field and droplet trajectories are calculated in turns the solution can become unstable. Each set of droplet trajectories will repel the next iteration of droplet trajectories to the opposite side of the domain. To prevent this under-relaxation is used when the volumetric space charge is updated.

### 3.4 Electric field

The governing equation for the electric potential is the Poisson equation, see equation (3). We implement this as a Eulerian “phase” which is transported exclusively through diffusion. The diffusion coefficient is  $\epsilon_0$ , and the charge-density acts as a source term. Two types of boundary conditions are used. For grounded or electrified surfaces a Dirichlet condition is used, and the surface potential is set to the applied voltage. For insulated surfaces a Neumann condition is used, and the normal derivative of the potential is set to zero.

## 4 CASE SETUP

The validation case is a simulation of a rotary bell sprayer, of a type typically used in automotive industry. The geometry, boundary conditions and parameters have been adapted from Domnick et al.<sup>[2, 8]</sup>. The sprayer is oriented vertically downward, and positioned 230 mm above a 1x1 m flat plate that serves as the target. The computational domain is box with sides of 2 m and a height of 0.7 m, enclosing the geometry as shown in figure 2.

### 4.1 Mesh

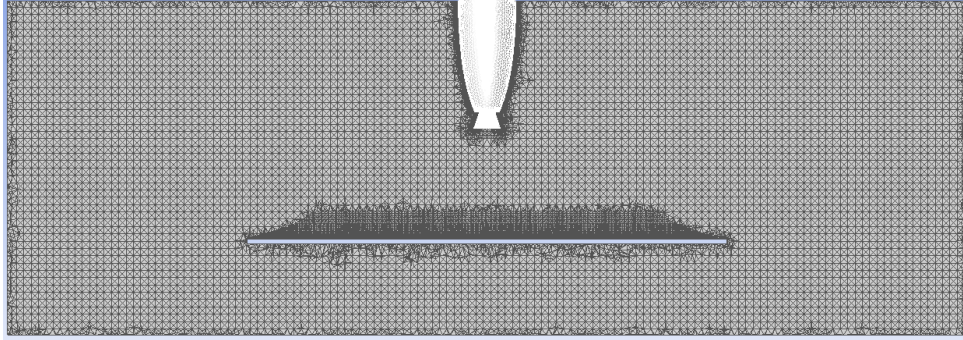


Figure 2: Cros section of the used mesh

An unstructured mesh with approximately 10 million elements was used for the validation simulation. The global element size is 10 mm, with refinement and inflation layers near the sprayer and target surface.

## 4.2 Boundary conditions

The top and bottom of the bounding box are treated as an inlet and an outlet respectively, creating a 0.3 m/s downwash around the sprayer. The sides of the bounding box are treated as symmetry conditions. All solid surfaces are treated as no-slip walls for the gas flow. Droplets impacting any solid surface are removed from the domain, while the total massflow of droplets is recorded in each surface element.

For the electric field, the target plate and the sprayer bell are treated as grounded and electrified respectively, with a constant electric potential. All other surfaces are considered to be insulated, i.e. the normal derivative of the potential being zero.

## 4.3 Sprayer and droplets

Primary and secondary breakup of the liquid near the sprayer is not modelled. Instead droplets are injected 1 mm outside the bell edge, equally distributed around the circumference with a  $\pm 0.5$  mm vertical stagger. A total of around 300000 droplet streams are tracked, with 22 different droplet sizes. The sprayer parameters are given in table 1, the used droplet size distribution is shown in figure 3.

Table 1: Sprayer parameters

Bell diameter	55 mm
Bell speed	45000 rpm
Liquid flow rate	90 ml/min
Sprayer voltage	70 kV
Droplet charge	$5\% * Q_R$
Droplet density	1000 kg/m <sup>3</sup>
Droplet surface tension	$35 * 10^{-3}$ N/m

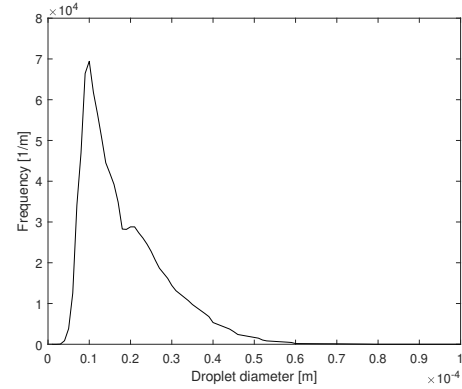


Figure 3: Size distribution of injected droplets

The droplet charge is based on the Rayleigh stability limit,  $Q_R$ , defined as equation (4).

$$Q_R = 8\pi \sqrt{\epsilon_0 \sigma r_p^3} \quad (4)$$

## 5 RESULTS

### 5.1 Validation simulation

Figure 4 shows a snapshot from the simulation results. The droplet trajectories are coloured according to mass, the electric potential is plotted on the symmetry plane and the target surface shows the accretion rate. This figure illustrates the complexity of the problem, as the droplet trajectories are wildly different depending on their size and charge. At small sizes, droplets are driven mostly by drag, at intermediate sizes by electrostatic force, and at large sizes inertia dominates their behaviour.

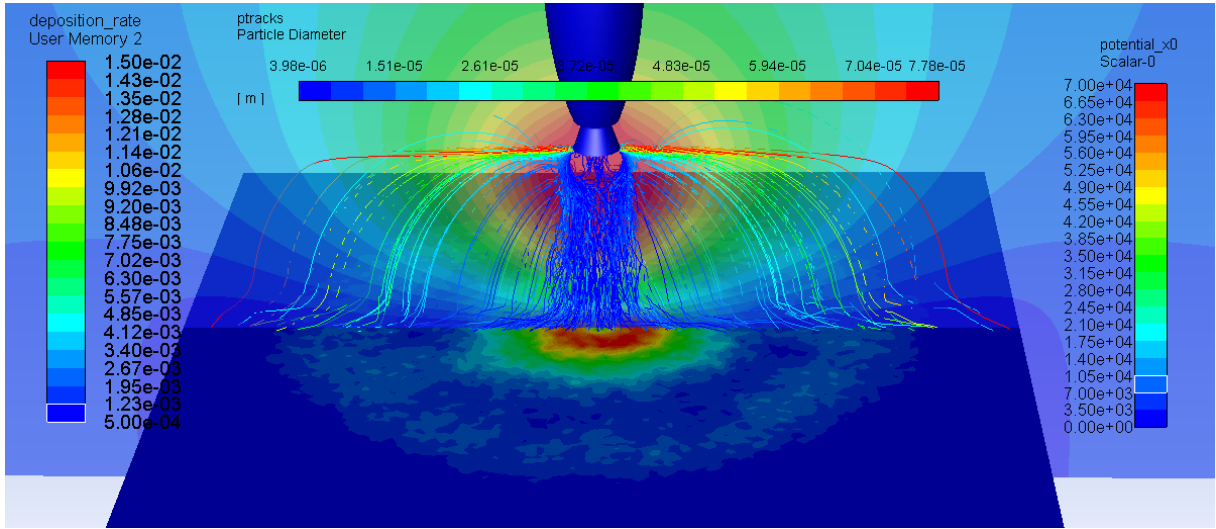


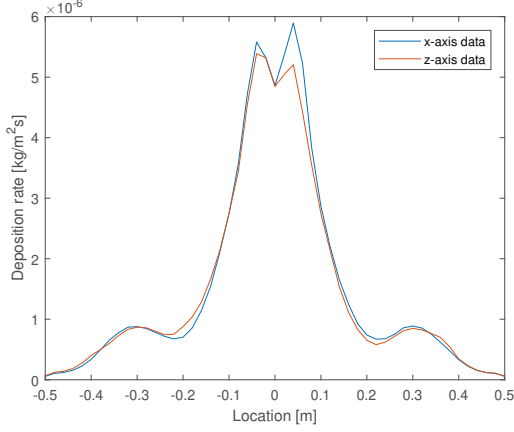
Figure 4: Droplet trajectories, electric field and accretion rate

The figure also shows a slightly asymmetric and irregular spray deposition pattern. This we attribute to a minor instability remaining in the simulation, and the fact that only a limited amount of particle trajectories can be calculated. To remedy this, the simulation was left to run for a total of 1000 cycles, the results of which were averaged, resulting in a smooth deposition pattern.

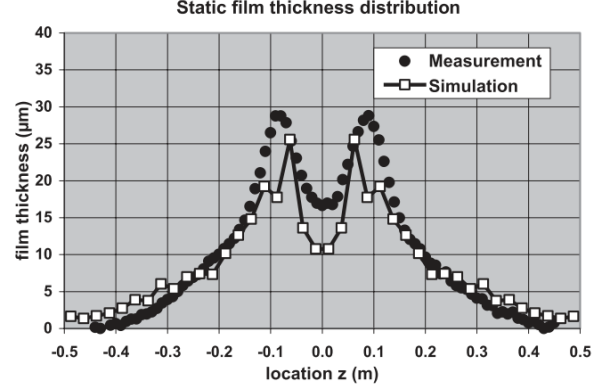
To compare our results with those obtained by Domnick et al.<sup>[2]</sup> the spray deposition rate was sampled along the middle of the target plate. The results are displayed in figures 5a (present simulation) and 5b (Domnick's, experimental and numerical). In our results two lines are plotted, representing sampling along both horizontal axes.

The experimental results adapted from Domnick et al.<sup>[2]</sup> were obtained by measuring the paint layer thickness obtained after an unspecified period of spraying. This makes quantitative comparison impossible, so only the overall profiles shapes may be compared. Doing so, several similarities and differences are apparent. In both cases the spray deposition tapers to near zero at the edges of the target plate, and has a local minimum at the centre. In our case the spray pattern forms an additional “ring”, with a local minimum around

200 mm from the sprayer axis. Not all boundary conditions could be retrieved from Domnick's work, which we expect is a reason for the observed mismatch.



(a) Deposition rate along centreline



(b) Paint deposition along centreline, adapted from Domnick et al.<sup>[2]</sup>

Figure 5: Comparison of simulation results with literature<sup>[2]</sup>

In general the simulation results match the experimental data, thus the model is extended to include the effects of evaporation.

## 5.2 Evaporation

To investigate the effects of including evaporation a new test case, which is more representative for our application, is constructed. It consists of cylinder placed inside a cubic box, with a cone-shaped spray aimed at the centre. Figure 6 shows a snapshot from a simulation of this case. An evaporation model based on Ranz and Marshall<sup>[9]</sup> is used. A free ion transport model is not used, meaning that the charge of evaporated droplets is completely removed from the domain.

When evaporation is included the general behaviour of the spray and the deposition pattern on the target do not change significantly. However, the total amount of fluid transferred to the target becomes highly dependent on the initial temperature and relative humidity. In addition, the results are highly sensitive to the droplet charge. In some cases with high charge and/or high spray mass flow the electric potential in the domain locally exceeds the sprayer voltage.

## 6 CONCLUSIONS

We succeeded in building a numerical model of an electrically charged spray using the Ansys Fluent (version 18) solver. With this model a stable solution could be found for several test cases. To validate the model we attempted to replicate the results obtained by Domnick et al.<sup>[2]</sup>. Our results did qualitatively agree with experimental data, although



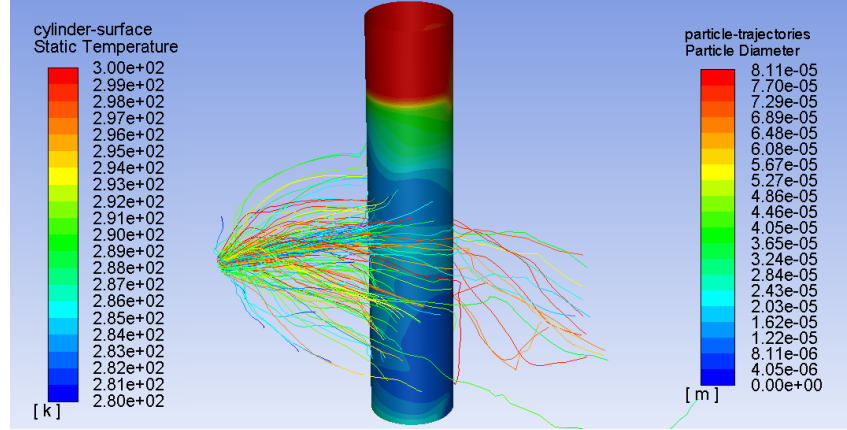


Figure 6: Evaporating spray, droplet trajectories coloured by diameter, target cylinder coloured by temperature

some differences were observed. We suspect these mostly come from the fact that some information regarding the geometry and operating conditions of the experimental setup was unavailable to us. Thus, despite the differences we conclude that our model produces accurate results, but foresee further validation efforts.

The present model has been expanded to include the effects of evaporation, which are necessary to model the application of charged sprays in a chilling warehouse. Initial simulations with evaporation modelling show promise, and the expected cooling effects are observed. Nevertheless, more work is necessary to include the exchange of charge between droplets and the continuous phase.

## NOMENCLATURE

$\epsilon_0$	Permittivity of the vacuum = $8.85 * 10^{-12}$ [F/m]
$\mu$	Gas dynamic viscosity [Pa.s]
$\Phi$	Electric potential [V]
$\rho$	Gas density [kg/m <sup>3</sup> ]
$\rho_p$	Droplet density [kg/m <sup>3</sup> ]
$\rho_q$	Charge density [C/m <sup>3</sup> ]
$\sigma$	Droplet surface tension [N/m]
$\vec{E}$	Electric field [V/m]
$\vec{g}$	Gravity vector [m/s <sup>2</sup> ]
$\vec{u}$	Gas velocity vector [m/s]
$\vec{u}_p$	Droplet velocity vector [m/s]

$C_D$	Droplet drag coefficient [-]
$d_p$	Droplet diameter [m]
$f_d$	Volumetric force applied by droplets on the airflow [N/m <sup>3</sup> ]
$p$	Pressure [Pa]
$q_p$	Droplet electric charge [C]
$Q_R$	Rayleigh stability limit for charged droplets [C]
$r_p$	Droplet radius [m]
$t$	Time coordinate [s]

## ACKNOWLEDGEMENTS

This work is supported by the EFRO Oost-Nederland programme within the CrestCool project (# PROJ-00730).

Furthermore, the authors would like to acknowledge Mr. Bert van Laer, as chair of the CrestCool project, and ir. Daan Laarman, both for fruitful discussions during our meetings.

## REFERENCES

- [1] A. G. Bailey, “Electrostatic spraying of liquids,” *Physics Bulletin*, vol. 35, pp. 146–148, apr 1984.
- [2] J. Domnick, A. Scheibe, and Q. Ye, “The Simulation of the Electrostatic Spray Painting Process with High-Speed Rotary Bell Atomizers. Part I: Direct Charging,” *Particle & Particle Systems Characterization*, vol. 22, no. 2, pp. 141–150, 2005.
- [3] V. Viti, J. Kulkarni, and A. Watve, “Computational Fluid Dynamics Analysis of the Electrostatic Spray Painting Process With a Rotating Bell Cup,” *Atomization and Sprays*, vol. 20, no. 1, pp. 1–17, 2010.
- [4] A. Mark, B. Andersson, S. Tafuri, K. Engstrom, H. Sorod, F. Edelvik, and J. S. Carlson, “Simulation of Electrostatic Rotary Bell Spray Painting in Automotive Paint Shops,” *Atomization and Sprays*, vol. 23, no. 1, pp. 25–45, 2013.
- [5] A. K. Arumugham-Achari, J. Grifoll, and J. Rosell-Llompart, “A Comprehensive Framework for the Numerical Simulation of Evaporating Electrosprays,” *Aerosol Science and Technology*, vol. 49, no. 6, pp. 436–448, 2015.
- [6] S. Arif, D. J. Branken, R. C. Everson, H. W. Neomagus, L. A. le Grange, and A. Arif, “CFD modeling of particle charging and collection in electrostatic precipitators,” *Journal of Electrostatics*, vol. 84, pp. 10–22, 2016.

- [7] B. Y. Guo, Y. B. Su, D. Yang, and A. B. Yu, “Predictions of the gasliquid flow in wet electrostatic precipitators,” *Applied Mathematical Modelling*, vol. 44, pp. 175–188, 2017.
- [8] J. Domnick, A. Scheibe, and Q. Ye, “The simulation of electrostatic spray painting process with high-speed rotary bell atomizers. Part II: External charging,” *Particle and Particle Systems Characterization*, vol. 23, no. 5, pp. 408–416, 2007.
- [9] W. E. Ranz and W. Jr. Marshall, “Evaporation from drops 1,2,” *Chemical Engineering Progress*, vol. 48, pp. 141–146, 01 1952.